

## Electronic Supplementary Information (ESI)

### Revisiting SrTiO<sub>3</sub> as a photoanode for water splitting: Development of thin films with enhanced charge separation under standard solar irradiation

Antonio N. Pinheiro<sup>a</sup>, Edney G. S. Firmiano<sup>a</sup>, Adriano C. Rabelo<sup>a</sup>, Cleocir J. Dalmaschio<sup>a</sup>, Edson R. Leite<sup>a</sup>

<sup>a</sup>Chemistry Department, Federal University of São Carlos

São Carlos, SP 13565-905 (Brazil)

email: [edson.leite@pq.cnpq.br](mailto:edson.leite@pq.cnpq.br)

The overpotential is defined as the potential difference (voltage) between a half-reactions reduction potential (thermodynamically determined) and the potential (redox event) experimentally observed [1].

However, in the water photoelectrolysis, the onset voltage for photocurrent ( $V_{on}$ ) under standard illumination condition is bellowing the  $1.23 V_{RHE}$ . Thus we can define a pseudo-overpotential as the difference between the onset voltage for photocurrent ( $V_{on}$ ) under standard illumination condition and the flat band potential ( $V_{fb}$ ), i.e.  $\eta_{OX} = V_{on} - V_{fb}$ . This definition is valid when the  $h^+$  diffusion length ( $L_p$ ) is much shorter than the depletion layer width ( $W_{SC}$ ) ( $L_p \ll W_{SC}$ ), and hence the photocurrent is primarily due to the carriers generated in the depletion layer.

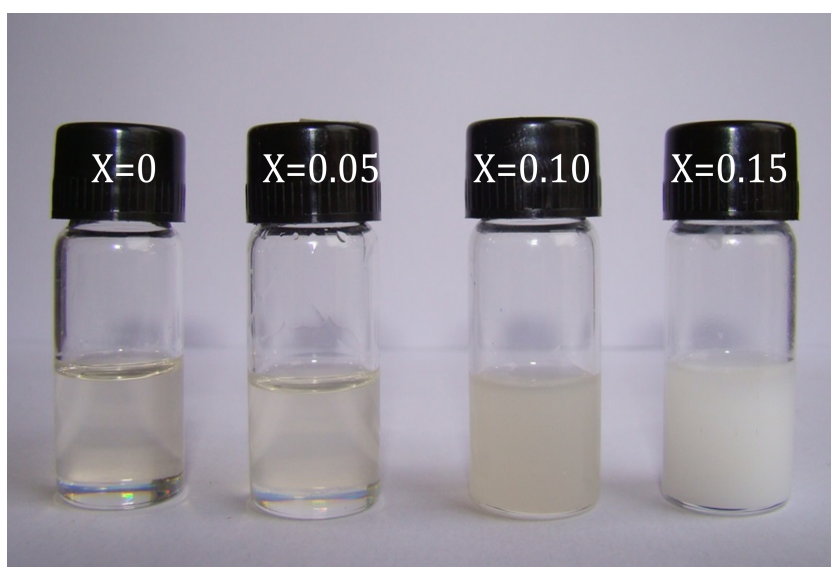


Figure S1 - Photograph of vials containing colloidal dispersion of SrTiO<sub>3</sub> nanoparticles doped with different Nb concentration. We can observe that the colloidal stability decrease with the increase of Nb.

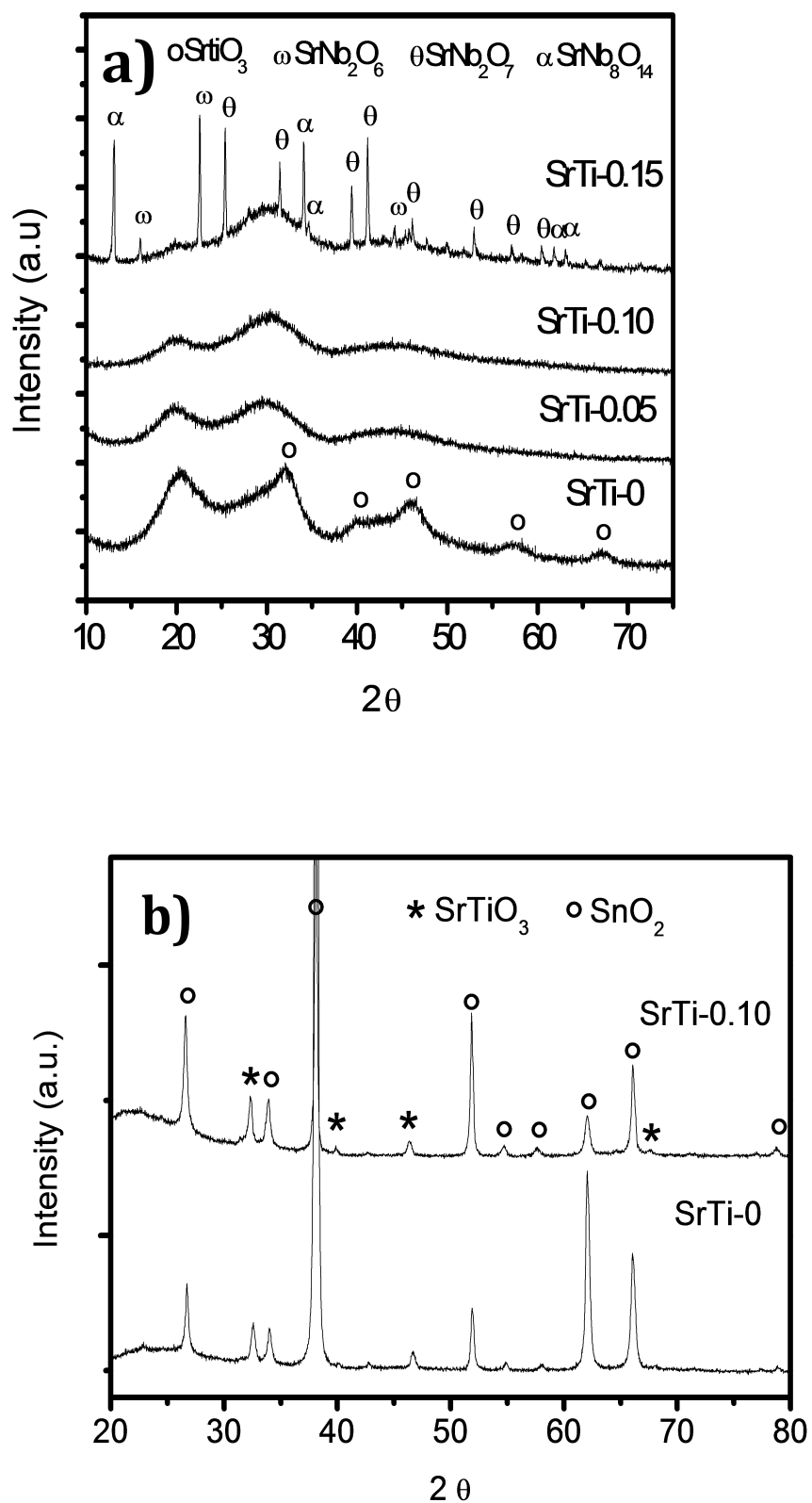


Figure S2 –a) XRD analysis of the as prepared SrTiO<sub>3</sub> nanoparticles doped with different Nb concentration; b) XRD analysis of the Nb-doped and undoped SrTiO<sub>3</sub> thin film (after sintering process).

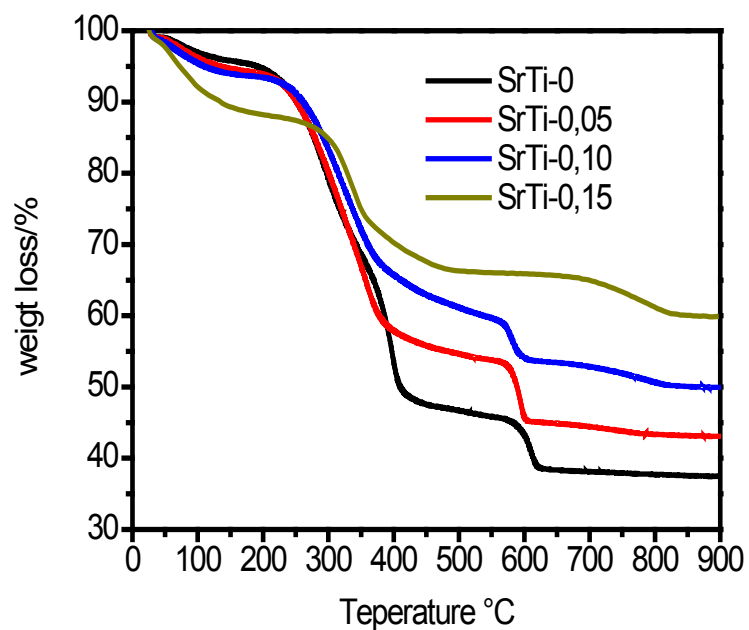


Figure S3 – Thermogravimetric analysis of the as prepared SrTiO<sub>3</sub> nanoparticles doped with different Nb concentration. Heating rate of 10°C/min.; atmosphere-O<sub>2</sub> flow.

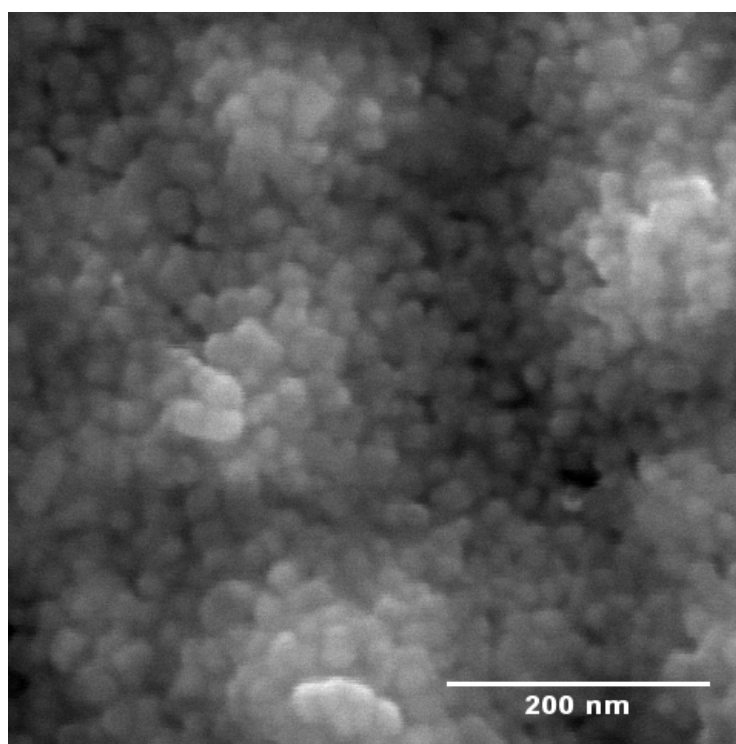


Figure S4 – High magnification in-lens secondary electron image of the STO sample

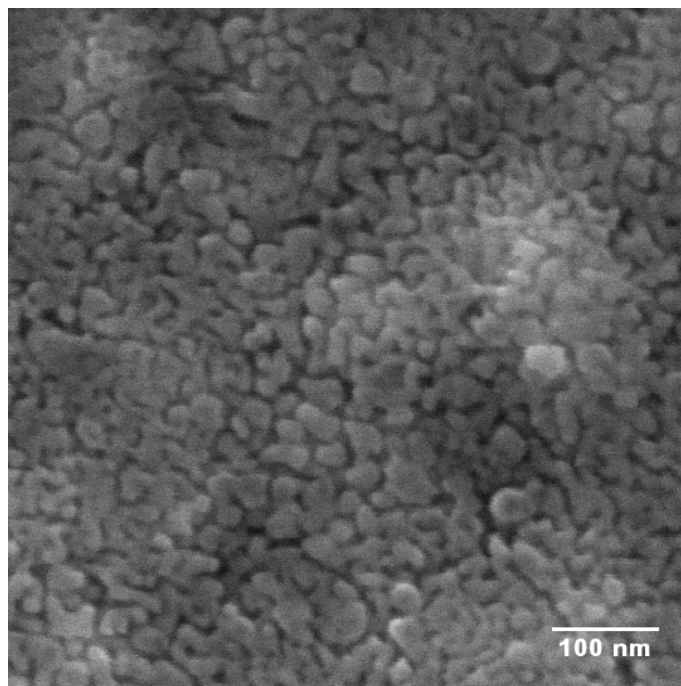


Figure S5 – High magnification in-lens secondary electron image of the Nb-STO sample

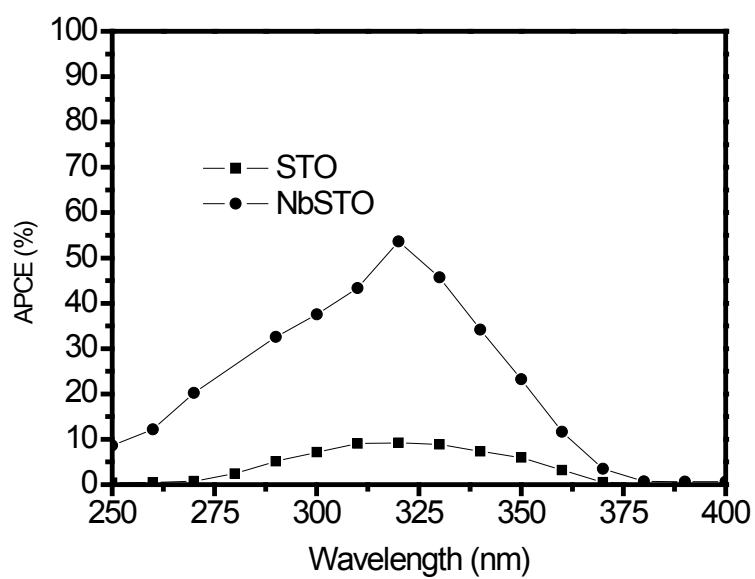


Figure S6 – APCE measurement of the Nb-STO and STO photoanodes under front illumination.

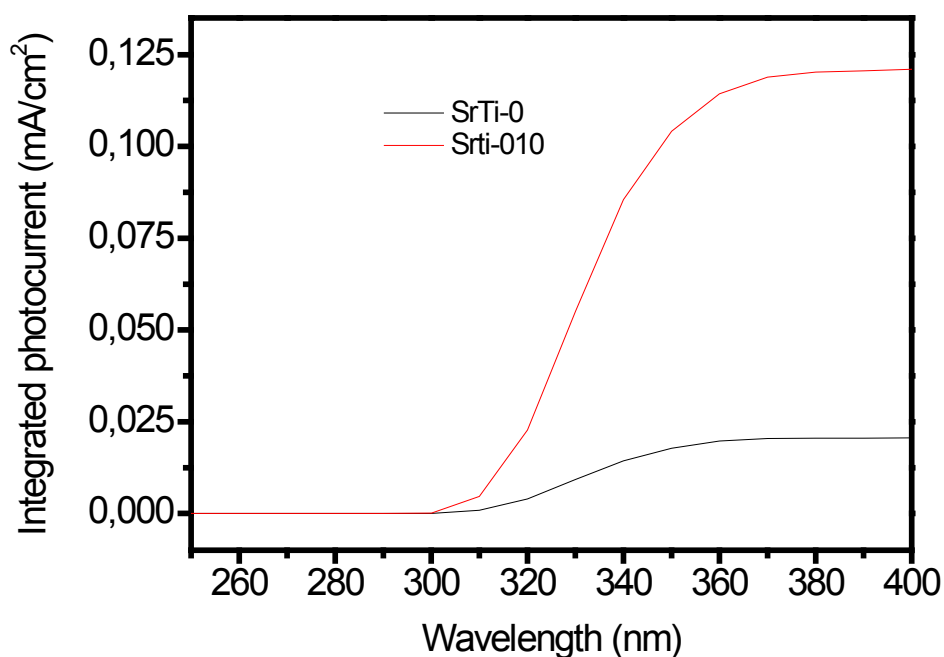


Figure S7 – Integrated solar photocurrent for IPCE data with the standard solar spectrum (AM 1.5/100 mW.cm<sup>-2</sup>), for the samples STO and Nb-STO.

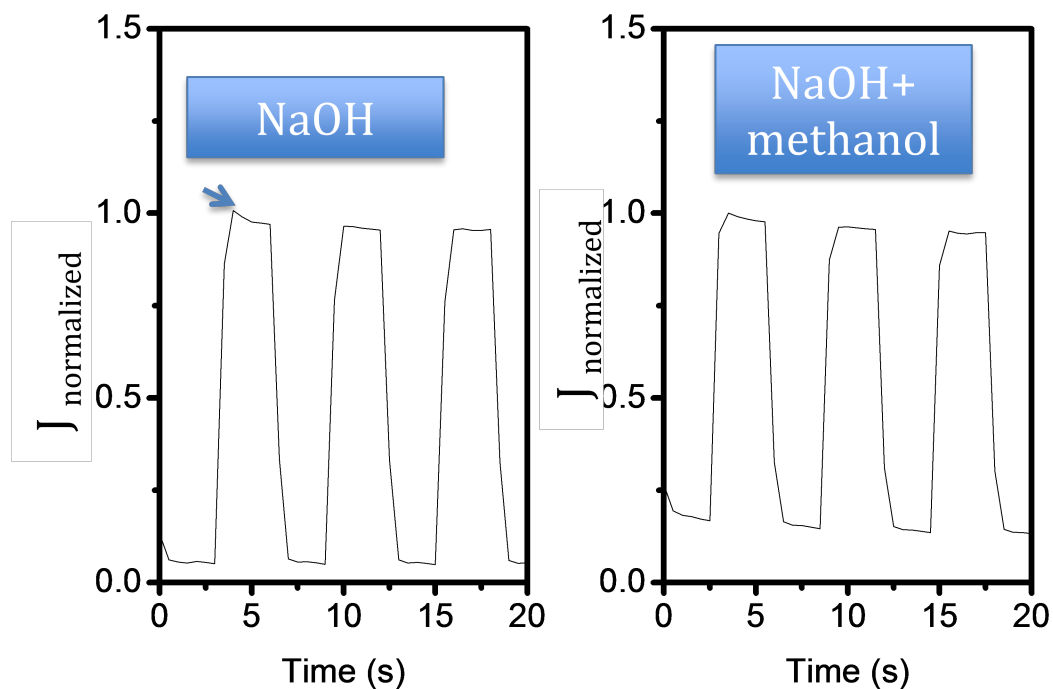


Figure S8 – Normalized Photocurrent ( $J/J_{Max}$ ) transient measurements performed at 0.3 V<sub>RHE</sub>, under standard solar illumination. The arrow indicate the spike.

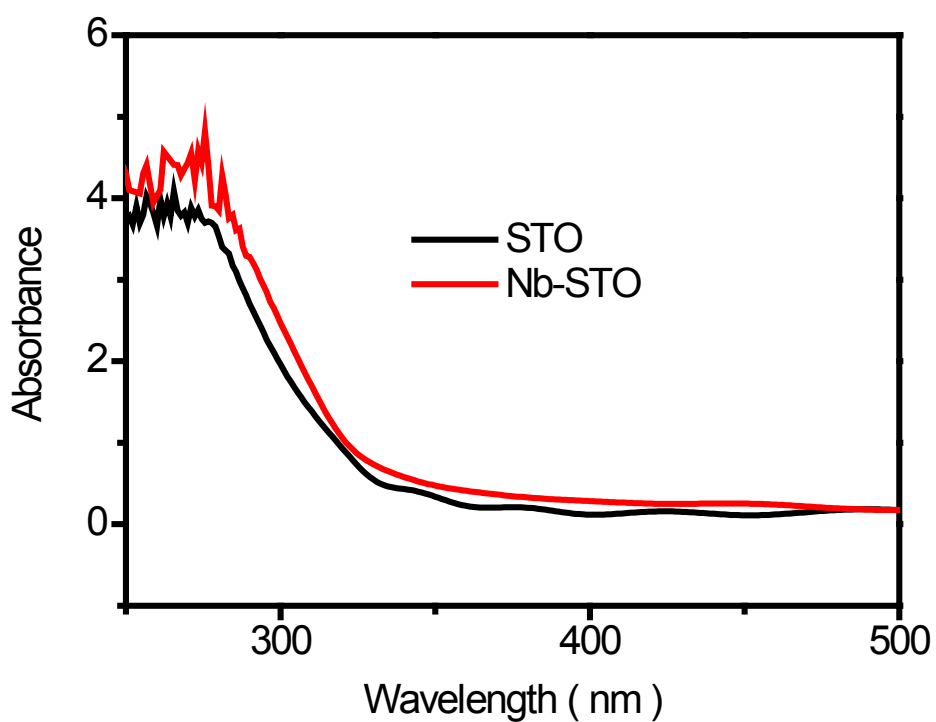


Figure S9 – UV-Vis absorption spectroscopy measurement for the STO and Nb-STO samples.

#### References

- [1] - Bard, A.J.; Faulkner, L.R. *Electrochemical Methods: Fundamentals and Applications*. New York: John Wiley & Sons, 2nd Edition, 2000.